accompanied by several serious adverse effects. Since cytokines play a pivotal role in immune reactions, application of cytokines has been extensively studied to control autoimmune diseases. Systemic administration of suppressive cytokines, such as transforming growth factor (TGF)-beta, interleukin (IL)-4, and IL-10 showed a significant efficacy in models of autoimmune diseases. Some of these agents seem to work by shifting the balance of immune deviation. However, systemic cytokine therapy potentially leads to deleterious side effects, as in the case of recombinant human IL-4.[2] On the other hand, cytokine-blocking therapies have been successful and will continue to serve as important strategies in many autoimmune diseases. However, because such strategies still have important drawbacks, including severe infections,[3] it will also be necessary to explore other specific immunotherapies.

Autoantigens for autoreactive T cells and autoantibodies have been extensively explored in various autoimmune diseases. These explorations are important not only for understanding the pathogeneses of autoimmune diseases, but also for establishing antigen-specific immunotherapies. If possible, suppression of the initial activation of antigen-specific T cells is feasible because intervention appears to be less effective on established pathogenic T cells. However, the majority of patients who require clinical treatment have full-blown autoimmune disease, and this approach would not be adequate. In advanced autoimmune diseases, an immune response to a single epitope on a self-antigen at the start of the disorder can trigger immune responses to adjacent epitopes on the same molecule or to other epitopes on related molecules. This phenomenon is called "epitope spreading." Although the precise impact of the epitope spreading is not evident in the entire autoimmune process, some researchers argue against antigen-specific immunotherapy because of the difficulties of predicting such expanding autoimmune reactions. However, we propose that epitope spreading is not the sole mechanism of the T cell–related pathogenesis of autoimmune diseases and that clonal restriction of T cells occurs in the late phase of autoimmunity. In this context, antigen-specific immunotherapy would be feasible, even for established autoimmune diseases. T cell receptor (TCR) gene transfer could be one of the possible strategies.

EVALUATION OF ANTIGEN-SPECIFIC T CELLS IN AUTOIMMUNE DISEASES

The model of epitope spreading or determinant spreading has been generally accepted in autoimmunity.[4,5] With respect to T cells, this is a diversification of specificity from the initial limited epitope-specific immune response to a hierarchical cascade of autoreactive T cell specificities. This model could explain the pathway of infection-induced autoimmunity. On the basis of this idea, the initial phase of the autoimmune reaction might be invoked by a few activated T cells against limited numbers of epitopes. These T cells may

be cross-reactive to both microbial epitopes and self-epitopes. On the other hand, in the late phase of the disorders, the reactive epitopes might spread and T cells recognizing a variety of different epitopes on the several different self-molecules would be activated. However, if epitope spreading is the only mechanism involved in the T cell immune responses in autoimmune disorders, development of effective antigen-specific immunotherapies will be difficult, because target epitopes and molecules will always have the potential to spread, and it would be difficult to define the pattern of spreading in a chronic human autoimmune disorder.

To verify the presence of epitope spreading throughout the autoimmune process, it is important to detect how specific T cells behave within the lymphocyte population in the pathological lesions. Previously, our group established a method to analyze accumulated T cell clones using RT-PCR and single-strand conformation polymorphism (SSCP) on TCR messages.[5] With this method, the same clones were found to exist in different joints, of an RA patient.[5,6] These results clearly suggested the uniformity of immune responses in RA throughout the arthritic lesions. In the case of HTLV-1 env-pX transgenic mice, which exhibit spontaneous symmetrical arthritis similar to human RA,[7] there were vigorous accumulations of T cells in the joints, but they were different among the different lesions in the early stage.[8] In the middle stage, several identical clones were accumulated in the different lesions. In the late stage, the majority of the accumulated clones exist uniformly in several arthritic lesions. The number of the dominant clones did not necessarily increase. These results in mice also suggested the relative uniformity of autoimmune responses in the pathological lesions.

We have observed similar clonal restriction in several spontaneous autoimmune animal models.[9,10] Moreover, oligoclonally expanded insulin-reactive T cells were identified in the pancreatic draining lymph nodes from type 1 diabetes patients with prolonged disease durations.[11] A limited T cell oligoclonality as a "driver clone" in autoimmunity was described in experimental autoimmune encephalomyelitis (EAE).[12,13] In polymyositis patients, several T cell clones persisted for several years in blood T lymphocytes and consecutive muscle biopsy specimens.[14] On the basis of these observations, we now speculate that epitope spreading does not necessarily work in the late phase of the disease progression, and it is possible that some form of clonal restriction of T cells occurs in autoimmune disorders. Some restricted T cell clones directed toward certain target self-antigens might be sustained. Avidity maturation of a pathogenic T cell population may be the decisive event in the progression of benign inflammation to full-blown autoimmune disease.[15] Therefore, it is feasible to suppress sustained pathologic responses without global immuosuppression.

In immune responses to foreign antigens, T cell responses are dominated by few clonotypes.[16] This clonal selection and dominance may be due to the competitive advantages of higher-affinity receptor, duration of TCR–pMHC

interaction, or affinity threshold.[17] In viral infections, clonal T cell "immunodomination" occurs in CD8+ T cells, probably because of proliferation advantages, differences of TCR affinity, or co-signal requirements.[18] Hence, the clonal restriction of T cells is not a behavior specific to these diseases, but can be considered as an universal phenomenon.

TCR GENE TRANSFER FOR CONTROLLING AUTOIMMUNE DISEASES

In the application of T cell targeted antigen-specific immunotherapy, there are several technical difficulties in the establishment of autoantigen-specific T cells. Usually the culture should be performed without the information of appropriate autoantigens. We have to select a candidate autoantigen in cloning culture of autoantigen-specific T cells based on the limited information. Moreover, there is no guarantee that *in vitro* established T cell clones represent real disease-associated T cells, mainly because *in vivo* activated T cells are more easily rendered in activation-induced cell death. Therefore, we attempted to produce inflammation-associated T cells by gene transfer of TCRs obtained *in vivo*.

Reconstitution of Antigen-Specific T Cells By TCR Gene Transfer

TCRs of the accumulated T cell clones in the inflammatory lesions can be visualized by RT-PCR/SSCP analysis. We attempted to obtain a pair of full-length cDNAs encoding alpha and beta chains of TCR expressed in a single cell in the lesion. We can reconstitute TCR function by expressing them with gene transfer to self T cells. For the gene transfer to lymphocytes, we have established a highly efficient retrovirus vector system with PLAT-E and pMX. PLAT-E is a packaging cell transfected gag–pol and env segment separately. Two independent monocistronic retrovirus vectors harboring alpha and beta TCR cDNAs were generated. For the first study, the class II MHC-restricted alpha and beta TCR genes specific for chicken OVA were used. These TCR genes were cloned from TCR transgenic mice designated DO11.10. These TCRs were transduced to splenocytes from BALB/c mice. The results indicated that alpha and beta TCR gene transfer into peripheral T cells reconstituted the antigen-specific immunity.[19] The amount of TCR expression and both the *in vitro* and *in vivo* antigen-specific functions were comparable to those obtained with splenocytes from DO11.10 transgenic mice. Moreover, DO11.10 TCR and IL-10-co-transduced CD4-positive T cells suppressed delayed type hypersensitivity to OVA, strongly compared to IL-10-transduced polyclonal CD4-positive T cells (Okamura *et al.*, unpublished observation).

Gene Therapy of a Model of Systemic Autoimmune Disease

We next attempted to use this TCR gene transfer to control autoimmune disorders. The target was lupus-prone NZB/W F1 mice, which spontaneously develop a lupus-like syndrome and nephritis. Anti-DNA antibodies are believed to be one of the major pathogenic autoantibodies for the nephritis. Datta and others have pointed out that nucleosome is a major immunogen in SLE.[20,21] Since DNA and nucleosome are physically associated, it is speculated that nucleosome-reactive T cells help the activation of anti-DNA-specific B cells as the hapten-carrier model. Therefore, we tried to generate nucleosome-specific T cells with an immunosuppressive function.[22] We selected CTLA4Ig as a suppressive molecule. TCR cDNAs were engineered on the basis of the published sequence of nucleosome-specific TCRs by fusing TCR V region sequence, synthesized CDR3 sequence, and TCR J-C region sequence. They were V alpha 13 and V beta 4. This TCR recognizes the immunodominant I-A^d-restricted nucleosomal epitope.

In our usual experimental protocol, the proportion of clonotypic TCR expression cells with two transferred TCR genes was estimated to be about 25% in CD4 + T cells. The introduction of TCR was found to reconstitute the specificity for the nucleosome. We then performed triple gene transfer together with CTLA4Ig to generate regulatory T cells (FIG. 1). Our calculations showed that approximately 10% of the total CD4-positive cells expressed all three genes. The CTLA4Ig secreted from transduced T cells blocked the proliferation of the polyclonal T cell population. The TCR and CTLA4Ig transduced cells showed the increase of CTLA4Ig secretion on T cell activation in the presence of DCs. A million of the nucleosome-specific regulatory T cells engineered by the triple genes were then transferred into 10-week-old NZB/W F1 mice. The mice were monitored for proteinuria. By week 22, all of the control mice that had received PBS, cells transferred with mock vectors, TCR alone, and CTLA4Ig started to develop severe nephritis diagnosed by the presence of persistent proteinuria of more than 300 mg/dL. By 30 weeks of age, the majority of these control mice showed severe proteinuria. However, none of the mice treated with cells transferred by the TCRs and CTLA4Ig showed excess proteinuria. The kidneys of the control mice showed severe glomerulonephritis with membranoproliferation, glomerular sclerosis, and tubular casts. The treated mice had mild glomerular disease with less deposition of IgG and complement, especially in the capillary loop. The autoantibodies usually found in NZB/W F1 mice were measured in the sera from different groups. The elevations of anti-dsDNA and anti-histone antibodies were suppressed at 22 weeks of age in the TCR and CTLA4Ig-treated mice. The T cell–dependent humoral response to active immunization of OVA was also analyzed. The level of anti-OVA IgG antibody titer was not significantly different from those of the control mice, indicating there was not an overt systemic immunosuppression of the triple gene-treated mice.

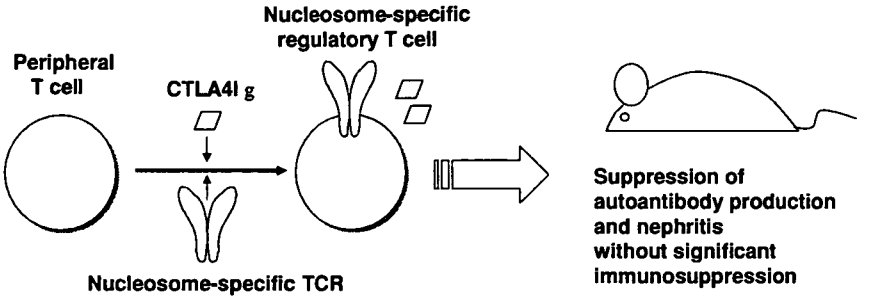

FIGURE 1. Experimental outlines of TCR gene transfer for systemic autoimmune diseases. Therapeutic effect of nucleosome-specific CTLA4Ig-producing T cells in lupus-prone NZB/W F1 mice is shown.

Gene Therapy of Arthritis with Inflamed Paw Homing TNFRIg-Producing T Cells

In order to obtain the whole TCR information from pathological lesions, we developed a method to clone a pair of full-length TCR cDNAs from a single cell accumulated in the inflamed joints of DBA/1 mice with collagen-induced arthritis.[23] Cloning of full-length cDNA encoding TCR was already established.[24] Single cell sorting with CD4+ and V beta 8.1/8.2-positive cells was performed and TCR messages were amplified with 3-step nested PCR using a fixed V beta primer and multiple V alpha primers. We then compared the clones obtained from the single cells with accumulated clones observed in the arthritic joints using the RT-PCR/SSCP method. Some TCRs from sorted single cells were actually identical to major accumulated clones in the joints. The full-length TCR cDNAs were subcloned into retrovirus vectors and transferred to DBA/1 splenocytes. Interestingly, some of the pairs of TCR were found to be not specific to immunized type II collagen, but reactive to self-antigen, because TCR-transferred cells proliferated in the culture with DCs from normal and arthritic mice. The carboxyfluorescein diacetate succinimidyl ester (CFSE)-labeling experiments showed that such TCR-transduced cells accumulated and proliferated in the arthritic joints. We next performed a therapeutic experiment using the triple gene-engineered T cells. In this experiment, soluble fusion protein of TNF receptor p75 and Fc domain of IgG2a (TNFRIg) was used as a regulatory molecule. We selected one of the TCR pairs, B47, which expanded in the arthritic paws. Control cells were transduced with either B47 alone or TNFRIg alone. In terms of the arthritis score as well as the incidence of severe arthritis, only B47 plus TNFRIg-transduced cells significantly suppressed the arthritis (FIG. 2A). Interestingly, the serum concentration of TNFRIg was not the main determinant of arthritis suppression in the B47+TNFRIg group, because the serum concentrations of TNFRIg protein in the B47+TNFRIg group were equivalent to those in the TNFRIg group. In contrast, the amount

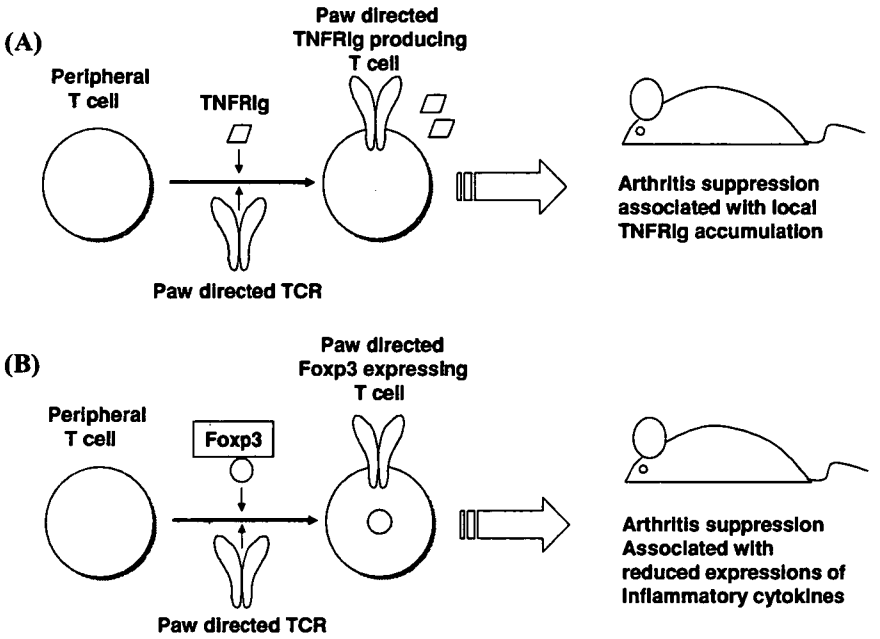

FIGURE 2. Experimental outlines of TCR gene transfer for collagen-induced arthritis. (**A**) and (**B**) illustrate therapeutic effect of paw-directed TNFRIg-producing T cells and paw-directed Foxp3-expressing T cells.

of TNFRIg in the paws of the B47+TNFRIg group was significantly higher than that in the paws of the TNFRIg group. Therefore, local accumulation of the TNFRIg transcript suppressed arthritis in the B47+TNFRIg group, and so biological agents producing T cells may have the advantage over the conventional biological agents that depend on serum concentration. A reduced serum concentration may be associated with less systemic immunosuppression.

Gene Therapy of Arthritis with Inflamed Paw Homing Foxp3-Expressing T Cells

Fopx3 is reported to be the key regulator for regulatory T cells. Several groups have reported that regulatory T cells are accumulated in the joints of arthritis patients.[25,26] Joint accumulating $CD4^+CD25^+$ T cells displayed an increased suppressive capacity compared with blood $CD4^+CD25^+$ T cells. However, the precise role of these accumulating regulatory T cells was not clarified in arthritis pathology. We generated B47+Foxp3 transduced cells and three groups of controlled gene transfer, Mcok, B47 alone and Foxp3 alone. The reconstituted regulatory T cell group, B47+Foxp3, significantly

suppressed the development of arthritis (FIG. 2B). The Foxp3-alone transduced group suppressed arthritis only marginally. The titers of anti-type II collagen antibodies were not different in these experimental groups. We next evaluated gene expression of inguinal lymph nodes and foot with quantitative PCR. Among cytokines important for arthritis progression, TNF-alpha, IL-17A, and IL-1beta were significantly suppressed. A suppressive cytokine, IL-10, was not upregulated in B47+Foxp3 group. In inguinal lymph nodes, the expression of TNF-alpha, IL-17A, and IL-1beta were not suppressed in B47+Foxp3 group. On histologic examination, although control groups showed severe inflammation, B47+Foxp3 group showed only marginal inflammation. We graded mononuclear cell infiltration and cartilage/bone destruction by the pannus invasion with histopathological examination. Pannus formation was clearly suppressed in the B47+Foxp3 group. These results suggest that regulatory T cells in the arthritis site suppress bone destruction as well as inflammation. In contrast, Foxp3-transduced T cells without antigen specificity were not sufficient for arthritis suppression. Reconstituted regulatory cells also showed effective suppression when transferred after the onset of arthritis when the average arthritic score reached around 2 point. Foxp3-expressing T cells with arthritis-associated TCRs were evidently effective in arthritis suppression. Once activated, regulatory T cells exhibit suppression in an antigen-nonspecific manner.[27] However, antigen specificity is important in migration and expansion of regulatory T cells.[28,29] Indeed, antigen-specific regulatory T cells are efficient in suppression of various autoimmune diseases. The problem is how to obtain enough organ-antigen-specific regulatory T cells for therapeutic transfer. TCR and Foxp3 gene transfer is one possible approach to overcome this problem. In the CIA treatment of polyclonal regulatory T cells, 20 mouse spleens were required to treat 1 mouse.[30] In contrast, about a quarter of splenocytes were used to treat one mouse in our experiment.

CONCLUSION

Taking these results together, the system illustrated in the FIGURE 2 was shown to be feasible for use in experimental animals. Recently, the clinical appreciation of retroviral TCR gene transfer was reported in the treatment of melanoma patients. T cells transduced with melanoma antigen-specific TCRs suppressed disease progression in patients with advanced melanoma.[31] This result showed the essential efficacy and safety of TCR gene transfer in the human. Therefore, autoimmune disease can be a suitable target for TCR gene transfer.

We propose that TCR gene cloning, using the information of TCR clonal analysis and reconstitution of the TCR function by gene transfer, would be a promising strategy for antigen-specific immunotherapy in autoimmune disorders.

ACKNOWLEDGMENTS

This work was supported by grants from the Japan Society for the Promotion of Science, Ministry of Health, Labor and Welfare and the Ministry of Education, Culture, Sports, Science and Technology of Japan.

REFERENCES

1. JACOBSON, D.L., S.J. GANGE, N.R. ROSE & N.M. GRAHAM. 1997. Epidemiology and estimated population burden of selected autoimmune diseases in the United States. Clin. Immunol. Immunopathol. **84:** 223–243.
2. LEACH, M.W., E.A. SNYDER, D.P. SINHA & I.Y. ROSENBLUM. 1997. Safety evaluation of recombinant human interleukine-4. I. Preclinical studies. Clin. Immunol. Immunopathol. **83:** 8–11.
3. OLSEN, N.J. & C.M. STEIN. 2004. New drugs for rheumatoid arthritis. N. Engl. J. Med. **350:** 2167–2179.
4. VANDERLUGT, C.L. & S.D. MILLER. 2002. Epitope spreading in immune-mediated diseses: implications for immunotherapy. Nat. Rev. Immunol. **2:** 85–95.
5. YAMAMOTO, K., K. MASUKO-HONGO, A. TANAKA, *et al.* 1996. Establishment and application of a novel T cell clonality analysis using single-strand conformation polymorphism of T cell receptor messenger signals. Human Immunol. **48:** 23–31.
6. YAMAMOTO, K., H. SAKODA, T. NAKAJIMA, *et al.* 1992. Accumulation of multiple T cell clonotypes in the synovial lesions of patients with rheumatoid arthritis revealed by a novel clonality analysis. Int. Immunol. **4:** 1219–1223.
7. IWAKURA, Y., M. TOSU, E. YOSHIDA, *et al.* 1991. Induction of inflammatory arthropathy resembling rheumatoid arthritis in mice transgenic for HTLV-1. Science **253:** 1026–1028.
8. KOBARI, Y., Y. MISAKI, K. SETOGUCHI, *et al.* 2004. T cell accumulating in the inflamed joints of spontaneous murine model of rheumatoid arthritis become restricted to common clonotypes during disease progression. Int. Immunol. **16:** 131–138.
9. KOMAGATA, Y., K. MASUKO, F. TASHIRO, *et al.* 1996. Clonal prevalence of T cells infiltrating into the pancreas of prediabetic non-obese diabetic mice. Int. Immunol. **8:** 807–814.
10. ZHOU, G., K. FUJIO, A. SADAKATA, *et al.* 2004. Identification of systemically expanded activated T cell clones in MRL/lpr and NZB/W F1 lupus model mice. Clin. Exp. Immunol. **136:** 448–455.
11. KENT, S.C., Y. CHEN, L. BREGOLI, *et al.* 2005. Expanded T cells from pancreatic lymph nodes of type 1 diabetic subjects recognize an insulin epitope. Nature **435:** 224–228.
12. VAN DEN ELZEN, P., J.S. MENEZES, A. AMETANI, *et al.* 2004. Limited clonality in autoimmunity: drivers and regulators. Autoimmunity Review **3:** 524–529.
13. HUANG, J.C., R.J. OBER & E.S. WARD. 2005. The central residues of a T cell receptor sequence motif are key determinants of autoantigen recognition in murine experimental autoimmune encephalomyelitis. Eur. J. Immunol. **35:** 299–304.

14. HOFBAUER, M., S. WIESENER, H. BABBE, *et al.* 2003. Clonal tracking of autoaggressive T cells in polymyositis by combining laser microdissection, single-cell PCR, and CDR3-spectratype analysis. Proc. Natl. Acad. Sci. USA. **100:** 4090–4095.
15. AMRANI, A., J. VERDGUER, S. SERRA, *et al.* 2000. Progression of autoimmune diabetes driven by avidity maturation of a T-cell population. Nature **406:** 739–742.
16. KEDZIERSKA, K., S.J. TURNER & P. DOHERTY. 2004. Conserved T cell receptor usage in primary and recall responses to an immunodominant influenza virus nucleoprotein epitope. Proc. Natl. Acad. Sci. USA **101:** 4942–4947.
17. MALHERBE, L., C. HAUSL, L. TEYTON & M.G. MCHEYZER-WILLIAMS. 2004. Clonal selection of helper T cells is determined by an affinity threshold with no further skewing of TCR binding properties. Immunity **21:** 669–679.
18. FACCHINETTI, A., S.D. SANTA, S. MEZZALIRA, *et al.* 2005. A large number of T lymphocytes recognize Moloney-murine leukemia virus-induced antigens, but a few mediate long-lasting tumor immunosurveillance. J. Immunol. **174:** 5398–5406.
19. FUJIO, K., Y. MISAKI, K. SETOGUCHI, *et al.* 2000. Functional reconstitution of class II MHC-restricted T cell immunity mediated by retroviral transfer of the alpha beta TCR complex. J. Immunol. **165:** 528–532.
20. MOHAN, C., S. ADEM, V. STANIK & S.K. DATTA. 1993. Nucleosome: a major immunogen for pathogenic autoantigen-inducing T cells of lupus. J. Exp. Med. **177:** 1367–1381.
21. KALIYAPERULAL, A., C. MOHAN, W. WU & S.K. DATTA. 1996. Nucleomosomal peptide epitope for nephritis-inducing T helper cells of murine lupus. J. Exp. Med. **183:** 2459–2469.
22. FUJIO, K., A. OKAMOTO, H. TAHARA, *et al.* 2004. Nucleosome-specific regulatory T cells engineered by triple gene transfer suppress a systemic autoimmune disease. J. Immunol. **173:** 2118–2125.
23. FUJIO, K., A. OKAMOTO, Y. ARAKI, *et al.* 2006. Gene therapy of arthritis with TCR isolated from the inflamed paw. J. Immunol. **177:** 8140–8147.
24. TAHARA, H., K. FUJIO, Y. ARAKI, *et al.* 2003. Reconstitution of CD8+ T cells by retroviral transfer of the TCR alpha beta-chain genes isolated from a clonally expanded P815-infiltrating lymphocyte. J. Immunol. **171:** 2154–2160.
25. VAN AMELSFORT, J. M., K.M. JACOBS, J.W. BIJLSMA, *et al.* 2004. CD4(+)CD25(+) regulatory T cells in rheumatoid arthritis: differences in the presence, phenotype, and function between peripheral blood and synovial fluid. Arthritis Rheum. **50:** 2775–2785.
26. DE KLEER, I.M., L.R. WEDDERBURN, L.S. TAAMS, *et al.* 2004. CD4+CD25bright regulatory T cells actively regulate inflammation in the joints of patients with the remitting form of juvenile idiopathic arthritis. J. Immunol. **172:** 6435–6443.
27. YU, P., R.K. GREGG, J.J. BELL, *et al.* 2005. Specific T regulatory cells display broad suppressive functions against experimental allergic encephalomyelitis upon activation with cognate antigen. J. Immunol. **174:** 6772–6780.
28. TANG, Q., K.J. HENRIKSEN, M. BI, *et al.* 2004. *In vitro*-expanded antigen-specific regulatory T cells suppress autoimmune diabetes. J. Exp. Med. **199:** 1455–1465.
29. TARBELL, K.V., S. YAMAZAKI, K. OLSON, *et al.* 2004. CD25+ CD4+ T cells, expanded with dendritic cells presenting a single autoantigenic peptide, suppress autoimmune diabetes. J. Exp. Med. **199:** 1467–1477.

30. MORGAN, M.E., R. FLIERMAN, L.M. VAN DUIVE NVOORDE, *et al.* 2005. Effective treatment of collagen-induced arthritis by adoptive transfer of CD25+ regulatory T cells. Arthritis Rheum. **52:** 2212–2221.
31. MORGAN, R.A., M.E. DUDLEY, J.R. WUNDERLICH, *et al.* 2006. Cancer regression in patients after transfer of genetically engineered lymphocytes. Science **314:** 126–129.

MOLECULAR AND CELLULAR BIOLOGY, July 2007, p. 5128–5134 Vol. 27, No. 14
0270-7306/07/$08.00+0 doi:10.1128/MCB.01072-06

CD3 and Immunoglobulin G Fc Receptor Regulate Cerebellar Functions[▽]

Kazuhiro Nakamura,[1]* Hirokazu Hirai,[2] Takashi Torashima,[2] Taisuke Miyazaki,[3] Hiromichi Tsurui,[1] Yan Xiu,[1] Mareki Ohtsuji,[1] Qing Shun Lin,[1] Kazuyuki Tsukamoto,[1] Hiroyuki Nishimura,[4] Masao Ono,[5] Masahiko Watanabe,[3] and Sachiko Hirose[1]

Department of Pathology, Juntendo University School of Medicine, Tokyo 113-8421, Japan[1]; Department of Neurophysiology, Gunma University Graduate School of Medicine, Maebashi, Gunma 371-8511, Japan[2]; Department of Anatomy, Hokkaido University School of Medicine, Sapporo 060-8638, Japan[3]; Department of Biomedical Engineering, Toin University of Yokohama, Yokohama 225-8502, Japan[4]; and Department of Pathology, Tohoku University Graduate School of Medicine, Sendai 980-8575, Japan[5]

Received 15 June 2006/Returned for modification 16 July 2006/Accepted 23 April 2007

The immune and nervous systems display considerable overlap in their molecular repertoire. Molecules originally shown to be critical for immune responses also serve neuronal functions that include normal brain development, neuronal differentiation, synaptic plasticity, and behavior. We show here that FcγRIIB, a low-affinity immunoglobulin G Fc receptor, and CD3 are involved in cerebellar functions. Although membranous CD3 and FcγRIIB are crucial regulators on different cells in the immune system, both CD3ε and FcγRIIB are expressed on Purkinje cells in the cerebellum. Both CD3ε-deficient mice and FcγRIIB-deficient mice showed an impaired development of Purkinje neurons. In the adult, rotarod performance of these mutant mice was impaired at high speed. In the two knockout mice, enhanced paired-pulse facilitation of parallel fiber-Purkinje cell synapses was shared. These results indicate that diverse immune molecules play critical roles in the functional establishment in the cerebellum.

Some molecules originally shown to be critical for immune responses, such as the major histocompatibility complex (MHC) class I molecules, CD3ζ, and semaphorin 7A (3, 8, 15, 23), also serve neuronal functions. Based on studies of mutant mice, CD3ζ proved critical for the development of lateral geniculate nucleus (LGN) and long-term synaptic plasticity in the adult hippocampus (3, 8).

In the immune system, CD3 subunits are expressed on T cells. The T-cell receptor (TCR)–CD3 complex recognizing specific antigens bound to MHC present on antigen-presenting cells (APCs) is composed of a TCR heterodimer and CD3 polypeptides organized as dimers. The cell-cell interaction between APCs and T cells is known as an immunological synapse (5) in the mature immune system. In αβ T cells, when the TCR interacts with the antigen/MHC complex, it transmits information to a signal-transducing complex consisting of two CD3 subunit dimers, CD3ε-CD3γ and CD3ε-CD3δ, and the CD3ζ-CD3ζ homodimer (10). Among CD3 subunits, CD3ζ is a crucial subunit having three immunoreceptor tyrosine-based activation motifs (ITAMs), whereas the remaining subunits have one ITAM (25). Tyrosine residues within these motifs are phosphorylated by src family tyrosine kinases, and then Src homology 2-containing proteins, including the tyrosine kinase ZAP70, participate in signaling (13). The signaling in γδ TCRs is different from that in αβ TCRs. Most γδ TCRs lack CD3δ, and signal transduction by γδ TCR is superior to that by αβ TCR, as measured by its ability to induce calcium mobilization, extracellular signal-regulated kinase activation, and cellular proliferation (6).

FcγRIIB is a low-affinity membrane receptor for immune complexes broadly distributed on hematopoietic cells, such as B cells, mast cells, basophils, macrophages, eosinophils, neutrophils, dendritic cells, and Langerhans cells. FcγRIIB negatively regulates B-cell receptor-induced signaling in B cells via the inhibitory immunoreceptor tyrosine-based inhibition motif in its cytoplasmic domain (24, 30). Coengagement of the B-cell receptor and FcγRIIB results in the tyrosine phosphorylation of the immunoreceptor tyrosine-based inhibition motif and the recruitment of SHIP. SHIP, by hydrolyzing PIP3, causes the dissociation of Brutons tyrosine kinase from the membrane and the inhibition of calcium influx into the cell (29). Although the functional significance of FcγRIIB has been elucidated in hematopoietic cells, the physiological roles of FcγRIIB have not been explored in the nervous system.

The cerebellum is a key region operating motor learning and motor coordination. Cerebellar functions are regulated by coordinated neural networks. There are two major types of inputs to the cerebellum: climbing fibers (CFs) and mossy fibers. CFs are the axons of neurons located in the inferior olive. They enter the cerebellum and establish two branches, one to the deep nuclei and one to the Purkinje cells (PCs) of the cerebellar cortex. Mossy fibers synapse with the claw-like dendrites of the granule cells (GCs) in the cerebellar cortex. The GCs in turn communicate with the PC dendrites via their long parallel fiber (PF) axons. PC axons are the sole efferents from the cerebellar cortex.

Here, we found an unexpected common functional significance of CD3 and FcγRIIB in the cerebellum. Both CD3ε and

* Corresponding author. Mailing address: Department of Pathology, Juntendo University School of Medicine, Tokyo 113-8421, Japan. Phone: 81-3-5802-1039. Fax: 81-3-3813-3164. E-mail: kaz@med.juntendo.ac.jp.

▽ Published ahead of print on 14 May 2007.

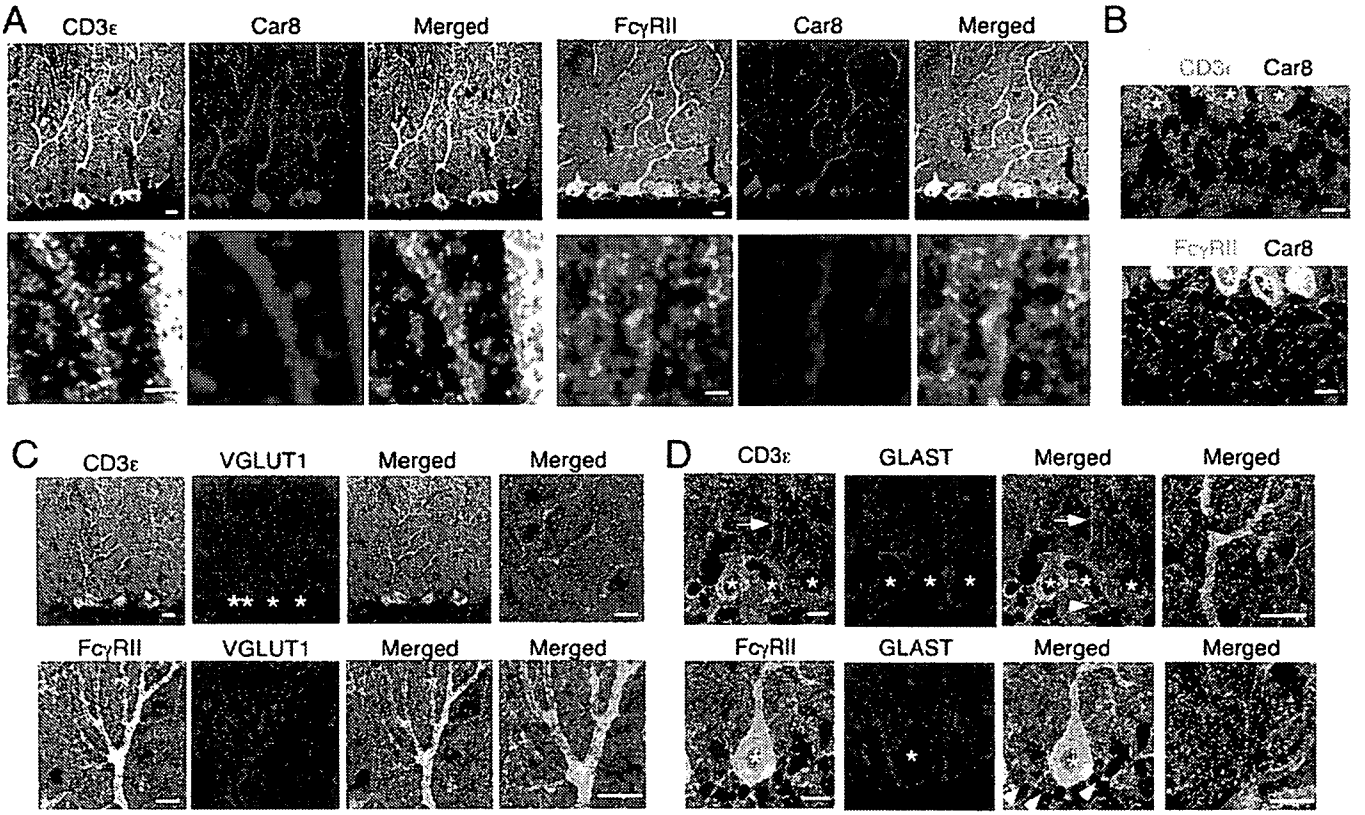

FIG. 1. Distribution of CD3ε and FcγRIIB in the cerebellum. Double immunofluorescence images are shown for CD3ε (green) or FcγRIIB (green) with Car8 (red) (A and B) in the molecular layer (A) and internal granular layer (B), with VGLUT1 (red) (C), or with GLAST (red) (D) in the cerebellum at P21. Arrows and arrowheads indicate rod-like staining of the Bergmann glia and the GLAST-positive cell bodies, respectively. Asterisks, Purkinje cell somata. Bars, 1 μm (A, lower panels) or 10 μm (A, upper panels, and B, C, and D).

FcγRIIB are located on Purkinje cells. CD3ε-deficient mice and FcγRIIB-deficient mice shared impaired development of Purkinje neurons, enhanced paired-pulse facilitation (PPF) of parallel fiber-Purkinje cell synapses, and poor rotarod performance at high speed.

MATERIALS AND METHODS

Animals. CD3ε knockout mice (16) with a C57BL/6 background were obtained from The European Mouse Mutant Archive. FcγRIIB knockout mice (30) with a C57BL/6 background were obtained from T. Takai (Tohoku Univ.). All animals were maintained according to the guidelines of Juntendo University.

RT-PCR. Reverse transcription-PCR (RT-PCR) was done using total RNA derived from the cerebellum and EL4 T-cell line and the following primers: *CD3ε* forward, 5′-AAGTCGAGGACAGTGGCTACTAC-3′, and reverse, 5′-CATCAGCAAGCCCAGAGTGATACA-3′; *CD3γ* forward, 5′-ATGGAGCAGAGGAAGGGTCTGGCT-3′, and reverse, 5′-CATTCTGTAATACACTTGCAGGGG-3′; *CD3δ* forward, 5′-GGAACAAATGTTGCTTGTCTGG-3′, and reverse, 5′-TCTTGGCAAACAGCAGTCGTA-3′; *CD3ζ* forward, 5′-AAGATGGCAGAAGCCTACAG-3′, and reverse, 5′-TTAATGACACAATGACCTTGC-3′; *CD3ζ* forward 5′-ACCCCAACCAGCTCTACAATGAG-3′, and reverse, 5′-AAGACGCTGGCACAGGATTGGCTA-3′. Primers for β-*actin* were purchased from Clontech (Palo Alto, CA).

Immunofluorescence staining. Immunofluorescence staining of the mouse cerebellum at postnatal day 21 (P21) was done essentially as described previously (20). The primary antibodies included anti-FcγRIIB (22), anti-CD3ε (145-2C11), anti-carbonic anhydrase 8 (Car8), anti-GLAST (26), anti-VGLUT1 (18), Alexa Fluor 488-labeled anticalbindin (Swant, Bellinzona, Switzerland), and Alexa Fluor 647-labeled anti-NeuN (Chemicon, Temecula, CA) antibodies. Anti-Car8 antibody was produced in the rabbit and guinea pig against 33 to 61 amino acid residues of the mouse Car8 (BC010773), and the specificity will be published elsewhere. Labeled sections were visualized with a confocal microscope (Zeiss LSM510). Quantitation of the pixel intensity of vGluT1 signals was carried out using Adobe PhotoShop and NIH Image.

Behavior. The performance on the rotarod (Ugo Basile, Comerio, Italy) was measured with a maximal observation time of 5 min. Animals were tested at a constant 5, 8, 10, or 30 rpm or an accelerating speed for two consecutive days, receiving four trials per day. The acceleration was started (2 rpm and the rod was rotating at ~30 rpm after 300 s), and the latency to fall was recorded.

Ambulation counts were made in an open field for 3 min essentially as described elsewhere (9). The behavioral tests were performed in a blind fashion.

Electrophysiology. Parasagittal cerebellar slices (200 μm) of the vermis were prepared from wild-type, FcγRIIB-deficient, and CD3ε-deficient mice (7). Slices were incubated at room temperature (25°C) for at least 1 h before recording. Whole-cell voltage clamp recordings were made of Purkinje cells visually identified at room temperature. The preparation was continuously superfused with an extracellular solution containing 124 mM NaCl, 2.5 mM KCl, 1.25 mM NaH_2PO_4, 1.5 mM $MgCl_2$, 2 mM $CaCl_2$, 26 mM $NaHCO_3$ and 20 mM glucose, which was bubbled continuously with a mixture of 95% O_2 and 5% CO_2. Patch pipettes had a resistance of 3 to 4 MΩ in the intracellular solution containing 135 mM Cs-D-gluconate, 15 mM CsCl, 1 mM $MgCl_2$, 10 mM HEPES, and 5 mM EGTA (pH 7.3). Picrotoxin (50 μM) was always present in the saline to block spontaneous inhibitory postsynaptic currents. To evoke PF or CF excitatory postsynaptic currents (EPSCs) from voltage-clamped Purkinje cells (−80 mV or 10 mV, respectively), square pulses (10 μs; 20 to 100 μA) were delivered every 10 s through a glass pipette with a tip 5 to 10 μm in diameter filled with 140 mM NaCl and 10 mM HEPES. To monitor the access resistance, a hyperpolarizing pulse (−10 mV; 50 ms) was applied 400 ms before the extracellular stimulation. Signals were filtered at 2 kHz and digitized at 4 kHz (Digidata 1320).

Statistics. Statistical significance was assessed using Student's *t* test unless otherwise noted. Analysis of variance was used for further analysis, and if there were significant differences, the Bonferroni test was used for post hoc analysis.

RESULTS

Expression of CD3ε and FcγRIIB in the developing cerebellum. We examined the distributions of CD3ε and FcγRIIB proteins in the mouse cerebellum at P21 by double immunofluorescence using cellular and subcellular markers. CD3ε and FcγRIIB proteins were distributed widely in the cerebellar cortex (Fig. 1). The most intense staining of CD3ε and FcγRIIB was found in perikarya and dendritic shafts of PCs, because each immunostaining showed considerable overlap with Car8 (Fig. 1A and B), a molecule known to be exclusive in PCs and responsible for ataxic mutant Waddles mice (11, 12). At a higher magnification, CD3ε and FcγRIIB were also detected in Car8-labeled dendritic spines of PCs (Fig. 1A, lower panels). Outside Car8-labeled PC elements, CD3ε and FcγRIIB were also distributed at low to moderate levels. To address these cellular elements, we used VGLUT1 and GLAST as a marker for parallel fiber terminals and Bergmann glia, respectively. Little, if any, CD3ε and FcγRIIB were detected in VGLUT1-labeled parallel fiber terminals (Fig. 1C), whereas they were found in GLAST-positive cell bodies and processes of Bergmann glia (Fig. 1D). A slight difference was also found in that CD3ε was detected in both Bergmann fibers (i.e., rod-like staining) (Fig. 1D) and lamellate processes (reticular staining in the neuropil), while FcγRIIB was preferentially seen in lamellate processes. Therefore, CD3ε and FcγRIIB are coexpressed in PCs and Bergmann glia in the cerebellar cortex.

Impaired cerebellar architecture in both CD3ε-deficient and FcγRIIB-deficient mice during development. In T cells, all CD3 subunits are assembled in the TCR-CD3 complex. The current model of TCR-CD3 signaling in T cells assumes coordinated regulation by all CD3 subunits. Phosphorylation of the ITAMs in CD3ζ is a critical step for actin polymerization, whereas the remaining CD3 subunits also participate in the signaling (5, 13). Therefore, we examined if the CD3 signaling machinery is established in the cerebellum. CD3γ and CD3δ transcripts were also found in the cerebellum at developmental stages. In contrast, CD3ζ mRNA was not detected at any stages of development using two sets of CD3ζ-specific primers (Fig. 2A), indicating that CD3 signaling components, such as CD3ε, CD3γ, and CD3δ, exist in the cerebellum, whereas the CD3 signaling seems to differ in the cerebellum from that in the immune system. Furthermore, CD3ε was preferentially expressed in the developmental stages. The CD3ε mRNA level was highest at P21. Therefore, we asked whether CD3ε and FcγRIIB contribute to the formation of neuronal architecture during development. We used two mutant mice, FcγRIIB-deficient mice and CD3ε-deficient mice, in which CD3δ is also not detected and the CD3γ protein level is reduced (16).

In the control mice, migrating NeuN-positive GCs with an ellipsoidal shape were observed at P7, whereas in the two mutant mice, these cells were round (Fig. 2B). Furthermore, when we quantified the area filled by GCs in IGL, a reduction was observed in the two knockout mice at both P3 and P7 (Fig. 2C). We then examined the development of PC dendrites. At P7, the size of the dendritic arbor and degree of branching of PCs were reduced in the two knockout mice compared to the control mice, as verified by calbindin staining (Fig. 2D). GCs extend PFs, and as the PFs extend, they make synaptic contact

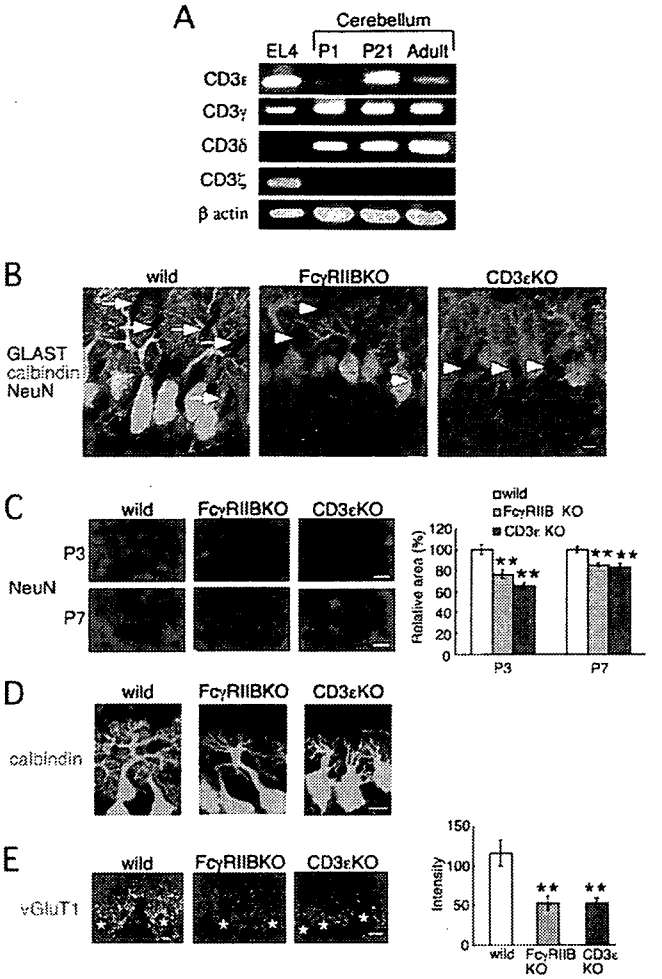

FIG. 2. Impaired neuronal architecture in FcγRIIB-deficient and CD3ε-deficient mice during cerebellar development. (A) RT-PCR analysis of each CD3 subunit in the EL4 T-cell line and the cerebellum from C57BL/6 mice at P1, P21, and the adult stage. β-Actin was used as the internal control. (B) Triple immunofluorescence for GLAST (red), calbindin (green), and NeuN (blue) at P7. Arrows and arrowheads indicate migrating GCs with an ellipsoidal shape and those with a round shape, respectively. (C) Immunofluorescence for NeuN at P3 and P7. The relative area occupied by granule cells was quantitatively compared. (D) Immunofluorescence for calbindin at P7. (E) The pixel intensity of VGLUT1 immunofluorescence was quantitatively compared. The left panel shows representative examples of immunofluorescence staining with anti-vGluT1 antibody at P7. The images were taken at the same exposure. Asterisks, Purkinje cell somata. Bars, 10 μm.

with the forming PC dendritic arbors. Synaptic terminals of PFs can be detected with anti-VGLUT1 antibody. In both mutant mice, the intensity of VGLUT1 signal was reduced at P7 (Fig. 2E).

CD3 and FcγRIIB have a common role in PF-PC synaptic function. Given the impaired development of PCs in the two mutant mice, we investigated whether these two molecules have common roles in synaptic functions in the adult by using electrophysiological approaches. We examined EPSCs in response to the stimulation of PFs or CFs in 8- to 10-week slice preparations by whole-cell patch clamping. There was no statistically significant difference in passive membrane properties between wild-type and FcγRIIB-deficient PCs (data not

TABLE 1. Basic properties of CF and PF EPSCs[a]

Synapse type	10–90% rise time[b] (ms)			Decay time constant[c] (ms)		
	Wild type	FcγRIIB KO	CD3ε KO	Wild type	FcγRIIB KO	CD3ε KO
CF EPSC	0.5 ± 0.1 (12)	0.5 ± 0.1 (15)	0.5 ± 0.1 (11)	14.1 ± 3.2 (12)	13.5 ± 3.6 (15)	12.7 ± 3.9 (11)
PF EPSC	2.7 ± 0.6 (15)	2.8 ± 0.7 (15)	2.7 ± 0.7 (15)	22.1 ± 5.5 (15)	22.5 ± 6.2 (15)	23.4 ± 5.7 (15)

[a] Data represent means ± standard deviations; *n* is reported in parentheses. KO, knockout.
[b] The time required for the synaptic current to increase from 10% to 90%.
[c] Current decay was fitted to single exponential curves.

shown). Basal transmission at PF-PC and CF-PC synapses was not significantly altered; there was no significant difference in either the rise or decay time constants of EPSCs between wild-type and FcγRIIB-deficient mice (Table 1). To investigate short-term synaptic plasticity, PPF at PF-PC synapses and paired-pulse depression (PPD) at CF-PC synapses were investigated by administering pairs of PF or CF stimuli at different interstimulus intervals. The PPF ratio was significantly increased in FcγRIIB-null slices when the interpulse interval was 20 to 220 ms: the PPF ratio at an interpulse interval of 20 ms was 205 ± 10% (mean ± standard error of the mean [SEM]) in wild-type mice and 259 ± 11% in FcγRIIB-deficient mice (Fig. 3A). In contrast, the PPD ratio was not significantly changed in FcγRIIB-deficient mice at interpulse intervals ranging from 20 to 3,000 ms (Fig. 3B).

Immature PCs are innervated by multiple CFs that originate from the inferior olive of the medulla (4). As animals grow, redundant CFs are gradually eliminated. FcγRIIB-deficient mice had almost the same percentage (more than 90%) of PCs innervated with a single CF as the wild-type mice (Fig. 3C),

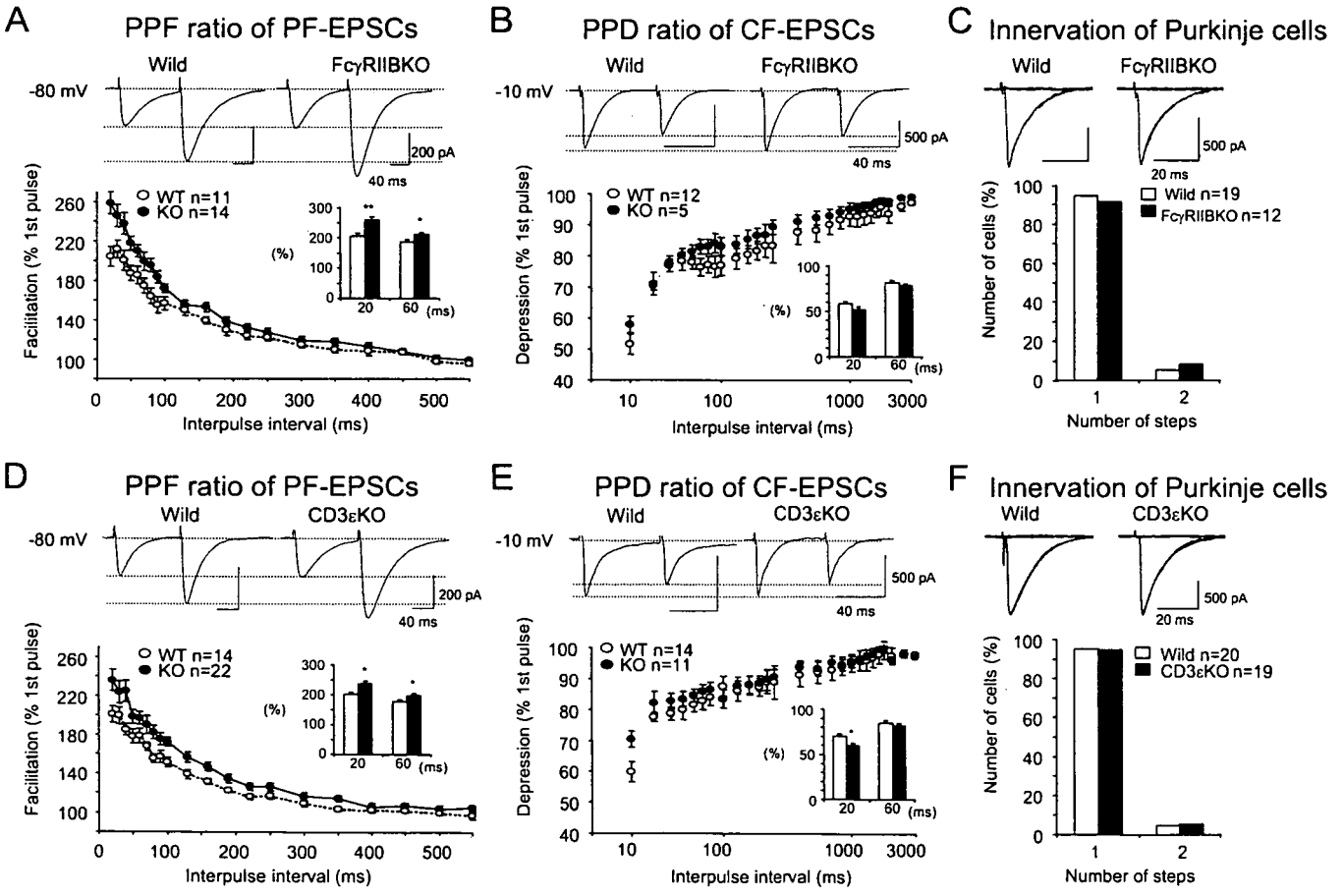

FIG. 3. Enhancement of PPF at PF-PC synapses in FcγRIIB-deficient and CD3ε-deficient mice. Short-term synaptic plasticity at PF- and CF-PC synapses was examined by applying pairs of stimuli separated by 20 to 550 ms or 20 to 3,000 ms. The second response (expressed as a percentage of the response to the first pulse; mean ± SEM) is plotted as a function of the interpulse interval. (A and D) PPF ratios of PF-EPSCs in FcγRIIB-deficient (A) and CD3ε-deficient (D) PCs were calculated. PF-EPSCs were obtained by holding membrane potentials at −80 mV. (B and E) PPD ratios of CF-EPSCs in FcγRIIB-deficient (B) and CD3ε-deficient (E) mice. (C and F) Single innervation of PCs by CFs in 8- to 10-week-old FcγRIIB-deficient (C) and CD3ε-deficient (F) mice. With gradually increasing stimulus intensities applied to the CFs, more than 90% of EPSCs of the wild-type and mutant mice were obtained in an all-or-none fashion. CF-EPSCs were elicited at −10 mV to inactivate voltage-dependent channels. Numbers of tested PCs (*n*) are indicated in each graph. *, $P < 0.05$.

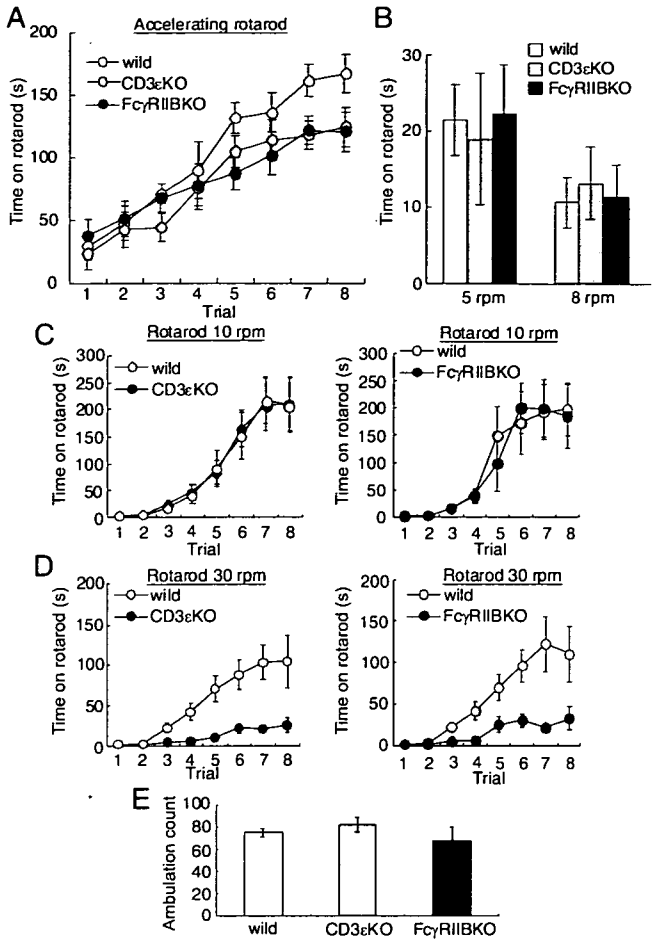

FIG. 4. Poor rotarod performance in FcγRIIB-deficient and CD3ε-deficient mice at high speed. (A) Amount of time mice remained on an accelerating rotarod over eight trials (n = 8 in each). (B) Amount of time mice remained on the rotarod at a constant 5 rpm or 8 rpm on the first trial (n = 8 in each). (C and D) Amount of time mice remained on the rotarod at a constant 10 rpm (n = 8 in each) (C) or 30 rpm (n = 7 in each) (D) over eight trials. (E) Ambulation count in the open field during 3 min (n = 6 to 7). Error bars represent the mean ± SEM.

thus indicating that the developmental elimination of surplus CF synapses on PCs was not impaired in the mutant mice.

Similar to FcγRIIB-deficient mice, the PPF ratio was significantly increased in CD3ε-deficient mice, while the PPD ratio was unchanged except at an interpulse interval of 20 ms (Fig. 3D and E). The developmental elimination of surplus CF synapses on PCs was not affected (Fig. 3F).

Poor rotarod performance in FcγRIIB-deficient and CD3ε-deficient mice. Finally, we assessed motor learning and motor coordination using the rotarod test in the two knockout mice. We first evaluated animals under standard conditions using an accelerating rotarod test (Fig. 4A). Rotarod speed increased from 2 rpm to 30 rpm within 5 min. On the first trial, the latencies at which the two mutant mice fell did not differ from those in the control mice. In all three strains, the latencies increased gradually as they gained experience (analysis of variance, $F_{7,\ 191} = 53.2$; $P < 0.0001$). As a whole, a strain effect did not reach a significant level ($F_{2,\ 191} = 2.3$; $P = 0.12$). However, the efficiency of improvements in the two mutant mice was lower in the latter four trials. During the first four trials, there was not a significant strain effect ($F_{2,\ 95} = 0.61$; $P = 0.55$). However, during the later four trials, a strain effect became evident ($F_{2,\ 95} = 7.0$; $P = 0.005$). Therefore, we hypothesized that the motor coordination evaluated in the first trial might not be changed, whereas the rising curve of the latency might be changed in the two mutant mice.

To confirm the hypothesis, we measured the latency in the first trial with constant rotarod speed. There were not significant differences at either 5 rpm or 8 rpm ($F_{2,\ 23} = 0.08$ [P = 0.93] and $F_{2,\ 23} = 0.12$ [P = 0.89], respectively) (Fig. 4B).

We next evaluated the rising curve of the latency at constant rotarod speed. When FcγRIIB-deficient and CD3ε-deficient mice were tested at a constant 10 rpm, they performed similarly to control mice ($F_{1,\ 103} = 0.02$ [P = 0.90] and $F_{1,\ 111}$ = 0.02 [P = 0.89], respectively) (Fig. 4C). In contrast, the latencies were significantly shorter in the FcγRIIB-deficient and CD3ε-deficient mice at 30 rpm ($F_{1,\ 127} = 28.7$ [P = 0.0001] and $F_{1,\ 127} = 20.1$ [P = 0.0005], respectively) (Fig. 4D). General motor activities in the two mutant mice, as evaluated by ambulation count in the open field, were not significantly changed ($F_{2,\ 21} = 0.98$, $P = 0.39$) (Fig. 4E). Thus, the rotarod performance was impaired at high speed.

DISCUSSION

In the present investigation, both CD3ε-deficient and FcγRIIB-deficient mice showed an increased PPF ratio in PF-PC synapses. PPF is an event characteristic of synapses with low release probability of a neurotransmitter. As the PF terminals mature, the release probability is increased, resulting in a decrease in the PPF ratio. Thus, an increased PPF in CD3ε-deficient and FcγRIIB-deficient mice indicates a lowered release probability of PF terminals. In these mutant mice, rotarod performances were worse only at high speed. The motor learning ability of these two mutant mice did not seem to be affected, because there were no differences at a low rotarod speed. In the FcγRIIB-deficient mice, robust long-term depression was induced following conjunctive stimulation of PFs with PC depolarization in the cerebellum (data not shown), which might reflect the selective impairment in rotarod tasks. In the two mutant mice, the upper limit of learning capacity might be lowered. However, we cannot exclude the possibility that the mutant mice have difficulty in gripping the rotarod at high speed. Interestingly, similar impairments, poor rotarod performance and mild enhancement of the PPF ratio in PF-PC synapses, were also seen in mutant mice deprived of Munc13-3, a component of presynaptic active zones (2). Further studies are needed to determine whether poor rotarod performance is associated with modification of PF-PC synaptic functions in these mutant mice.

We found impaired architectures of PCs and GCs during development in the two mutant mice. The two molecules are expressed on the somata, dendrites, and spines of PCs. Lack of either of the two molecules on PCs might intrinsically contribute to the impaired development of PC dendrites. Presynaptic terminals of PFs make synaptic contacts with PC dendrites, and PFs exert instructive roles in the development of distal PC dendrites and in the planar organization of dendritic arbors. We found lesser VGLUT1 signals in the two mutant mice.

Therefore, the immature GC might also contribute to the impaired PC dendrites.

The two molecules were also found on the Bergmann glia. An increasing body of evidence suggests the participation of Bergmann glia in the development of cerebellar neurons as a scaffold for the migration and positioning of cerebellar neurons (31). It is also possible that the two molecules on the Bergmann glia influenced the development of cerebellar neurons. However, the size of cultured astrocytes from the two mutant mice was not essentially altered compared to the control mice (data not shown).

We describe a role of immune molecules in the cerebellum in vivo. In the immune system, the two molecules are expressed in different immune cells. CD3ε is exclusively expressed on T cells, where the TCR-CD3 complex recognizes specific antigens bound to MHC on APCs and forms immunological synapses. Among CD3 subunits, roles of CD3ζ in the brain have been studied in vivo. CD3ζ is expressed in neurons, such as the LGN and hippocampus (3, 8). In CD3ζ mutant mice, refinement of connections between the retina and central targets during development was incomplete. These results indicate a crucial role for CD3ζ in functional weakening and structural retraction of synaptic connections in the LGN and hippocampus (3, 8). On the other hand, we showed unexpected roles of CD3ε, -γ, and/or -δ in the cerebellum because we used CD3ε-deficient mice, in which CD3δ is also not detected, and the CD3γ protein level was reduced (16). Our results and those with CD3ζ mutant mice suggest that the ligand for CD3 subunits exists in the brain. It remains elusive whether a common molecule acts as a ligand for both CD3ζ and other CD3 subunits. Recently, paired immunoglobulin-like receptor B (PirB), an MHC class I receptor, was found to be expressed in subsets of neurons throughout the brain, and in mutant mice lacking functional PirB, cortical ocular dominance plasticity is more robust at all ages (27). Although antigen/MHC complex is the ligand of the TCR-CD3 complex in T cells, it seems to be unlikely that MHC antigen is a ligand for CD3ε, -γ, and/or -δ in the cerebellum, because mice lacking surface expression of MHC class I and MHC class II knockout mice performed normally in a rotarod test (data not shown), and the TCRα transcript was not detected in the brain (21, 28). Unlike in the LGN and hippocampus, CD3ζ is absent in the cerebellum. The current model of TCR-CD3 signaling in T cells assumes phosphorylation of the ITAMs in CD3ζ and subsequent involvement of several molecules, such as ZAP-70, SLP76, Vav, Nck, and WASP, for actin polymerization (13). Therefore, other molecules might associate with CD3ε, -γ, and/or -δ in the cerebellum. FcRγ was a candidate because it has an ITAM and is included in the CD3 complex in T cells in the intestine of CD3ζ knockout mice (14, 17). However, the performances of FcRγ knockout mice in the rotarod test were comparable with those of control mice (data not shown). Rather, ITAM-independent signaling would function in the cerebellum.

FcγRIIB shows a different pattern of expression than CD3 in the immune system. FcγRIIB is broadly distributed on hematopoietic cells (29) but not on mature T cells. In immune cells, it inhibits various cellular functions, such as B-cell activation, antigen presentation, cell proliferation, and antibody production (29). FcγRIIB might also reduce the development of autoimmune disease. The lack of FcγRIIB enhanced susceptibility to myelin oligodendrocyte glycoprotein-induced autoimmune experimental allergic encephalitis and increased the extent of demyelination (1). Thus, the functions of FcγRIIB are different from those of CD3 in the immune system. In contrast, we demonstrated a common physiological role of the two molecules in the development of the cerebellum. FcRγ, another immunoglobulin G Fc receptor subunit, is pivotal to the differentiation of oligodendrocyte precursor cells into myelinating oligodendrocytes (19). Therefore, the roles of immunoglobulin G Fc receptors in the development of the brain are diverse. Further studies will elucidate the neuron-specific signaling of FcγRIIB and CD3.

ACKNOWLEDGMENTS

FcγRIIB knockout mice were kindly provided by T. Takai (Tohoku University).

We declare that none of the authors has financial interests.

This work was supported in part by research grants from the Ministry of Education, Science, Technology, Sports and Culture of Japan.

REFERENCES

1. **Abdul-Majid, K. B., A. Stefferl, C. Bourquin, H. Lassmann, C. Linington, T. Olsson, S. Kleinau, and R. A. Harris.** 2002. Fc receptors are critical for autoimmune inflammatory damage to the central nervous system in experimental autoimmune encephalomyelitis. Scand. J. Immunol. **55**:70–81.
2. **Augustin, I., S. Korte, M. Rickmann, H. A. Kretzschmar, T. C. Sudhof, J. W. Herms, and N. Brose.** 2001. The cerebellum-specific Munc13 isoform Munc13-3 regulates cerebellar synaptic transmission and motor learning in mice. J. Neurosci. **21**:10–17.
3. **Corriveau, R. A., G. S. Huh, and C. J. Shatz.** 1998. Regulation of class I MHC gene expression in the developing and mature CNS by neural activity. Neuron **21**:505–520.
4. **Crepel, F., J. Mariani, and N. Delhaye-Bouchaud.** 1976. Evidence for a multiple innervation of Purkinje cells by climbing fibers in the immature rat cerebellum. J. Neurobiol. **7**:567–578.
5. **Dustin, M. L., and J. A. Cooper.** 2000. The immunological synapse and the actin cytoskeleton: molecular hardware for T cell signaling. Nat. Immunol. **1**:23–29.
6. **Hayes, S. M., and P. E. Love.** 2002. Distinct structure and signaling potential of the gamma delta TCR complex. Immunity **16**:827–838.
7. **Hirai, H., T. Launey, S. Mikawa, T. Torashima, D. Yanagihara, T. Kasaura, A. Miyamoto, and M. Yuzaki.** 2003. New role of δ2-glutamate receptors in AMPA receptor trafficking and cerebellar function. Nat. Neurosci. **6**:869–876.
8. **Huh, G. S., L. M. Boulanger, H. Du, P. A. Riquelme, T. M. Brotz, and C. J. Shatz.** 2000. Functional requirement for class I MHC in CNS development and plasticity. Science **290**:2155–2159.
9. **Ichihara, K., T. Nabeshima, and T. Kameyama.** 1993. Dopaminergic agonists impair latent learning in mice: possible modulation by noradrenergic function. J. Pharmacol. Exp. Ther. **264**:122–128.
10. **Jacobs, H.** 1997. Pre-TCR/CD3 and TCR/CD3 complexes: decamers with differential signalling properties? Immunol. Today **18**:565–569.
11. **Jiao, Y., J. Yan, Y. Zhao, L. R. Donahue, W. G. Beamer, X. Li, B. A. Roe, M. S. Ledoux, and W. Gu.** 2005. Carbonic anhydrase-related protein VIII deficiency is associated with a distinctive lifelong gait disorder in waddles mice. Genetics **171**:1239–1246.
12. **Kato, K.** 1990. Sequence of a novel carbonic anhydrase-related polypeptide and its exclusive presence in Purkinje cells. FEBS Lett. **271**:137–140.
13. **Lin, J., and A. Weiss.** 2001. T cell receptor signalling. J. Cell Sci. **114**:243–244.
14. **Liu, C. P., R. Ueda, J. She, J. Sancho, B. Wang, G. Weddell, J. Loring, C. Kurahara, E. C. Dudley, A. Hayday, et al.** 1993. Abnormal T cell development in CD3-$\zeta^{-/-}$ mutant mice and identification of a novel T cell population in the intestine. EMBO J **12**:4863–4875.
15. **Loconto, J., F. Papes, E. Chang, L. Stowers, E. P. Jones, T. Takada, A. Kumanovics, K. Fischer Lindahl, and C. Dulac.** 2003. Functional expression of murine V2R pheromone receptors involves selective association with the M10 and M1 families of MHC class Ib molecules. Cell **112**:607–618.
16. **Malissen, M., A. Gillet, L. Ardouin, G. Bouvier, J. Trucy, P. Ferrier, E. Vivier, and B. Malissen.** 1995. Altered T cell development in mice with a targeted mutation of the CD3-epsilon gene. EMBO J. **14**:4641–4653.
17. **Malissen, M., A. Gillet, B. Rocha, J. Trucy, E. Vivier, C. Boyer, F. Kontgen, N. Brun, G. Mazza, E. Spanopoulou, et al.** 1993. T cell development in mice lacking the CD3-zeta/eta gene. EMBO J **12**:4347–4355.
18. **Miyazaki, T., M. Fukaya, H. Shimizu, and M. Watanabe.** 2003. Subtype

switching of vesicular glutamate transporters at parallel fibre-Purkinje cell synapses in developing mouse cerebellum. Eur. J. Neurosci. 17:2563–2572.
19. **Nakahara, J., K. Tan-Takeuchi, C. Seiwa, M. Gotoh, T. Kaifu, A. Ujike, M. Inui, T. Yagi, M. Ogawa, S. Aiso, T. Takai, and H. Asou.** 2003. Signaling via immunoglobulin Fc receptors induces oligodendrocyte precursor cell differentiation. Dev. Cell 4:841–852.
20. **Nakamura, M., K. Sato, M. Fukaya, K. Araishi, A. Aiba, M. Kano, and M. Watanabe.** 2004. Signaling complex formation of phospholipase Cβ4 with metabotropic glutamate receptor type 1α and 1,4,5-trisphosphate receptor at the perisynapse and endoplasmic reticulum in the mouse brain. Eur. J. Neurosci. 20:2929–2944.
21. **Nishiyori, A., Y. Hanno, M. Saito, and Y. Yoshihara.** 2004. Aberrant transcription of unrearranged T-cell receptor beta gene in mouse brain. J Comp. Neurol. 469:214–226.
22. **Ono, M., H. Okada, S. Bolland, S. Yanagi, T. Kurosaki, and J. V. Ravetch.** 1997. Deletion of SHIP or SHP-1 reveals two distinct pathways for inhibitory signaling. Cell 90:293–301.
23. **Pasterkamp, R. J., J. J. Peschon, M. K. Spriggs, and A. L. Kolodkin.** 2003. Semaphorin 7A promotes axon outgrowth through integrins and MAPKs. Nature 424:398–405.
24. **Ravetch, J. V., A. D. Luster, R. Weinshank, J. Kochan, A. Pavlovec, D. A. Portnoy, J. Hulmes, Y. C. Pan, and J. C. Unkeless.** 1986. Structural heterogeneity and functional domains of murine immunoglobulin G Fc receptors. Science 234:718–725.
25. **Reth, M.** 1989. Antigen receptor tail clue. Nature 338:383–384.
26. **Shibata, T., K. Yamada, M. Watanabe, K. Ikenaka, K. Wada, K. Tanaka, and Y. Inoue.** 1997. Glutamate transporter GLAST is expressed in the radial glia-astrocyte lineage of developing mouse spinal cord. J. Neurosci. 17:9212–9219.
27. **Syken, J., T. Grandpre, P. O. Kanold, and C. J. Shatz.** 2006. PirB restricts ocular-dominance plasticity in visual cortex. Science 313:1795–1800.
28. **Syken, J., and C. J. Shatz.** 2003. Expression of T cell receptor beta locus in central nervous system neurons. Proc. Natl. Acad. Sci. USA 100:13048–13053.
29. **Takai, T.** 2002. Roles of Fc receptors in autoimmunity. Nat. Rev. Immunol. 2:580–592.
30. **Takai, T., M. Ono, M. Hikida, H. Ohmori, and J. V. Ravetch.** 1996. Augmented humoral and anaphylactic responses in Fc gamma RII-deficient mice. Nature 379:346–349.
31. **Yamada, K., M. Fukaya, T. Shibata, H. Kurihara, K. Tanaka, Y. Inoue, and M. Watanabe.** 2000. Dynamic transformation of Bergmann glial fibers proceeds in correlation with dendritic outgrowth and synapse formation of cerebellar Purkinje cells. J. Comp. Neurol. 418:106–120.

Genetic Epidemiology 31: 709–726 (2007)

A Novel Method to Express SNP-Based Genetic Heterogeneity, Ψ, and Its Use to Measure Linkage Disequilibrium for Multiple SNPs, D_g, and to Estimate Absolute Maximum of Haplotype Frequency

Ryo Yamada* and Fumihiko Matsuda

Center for Genomic Medicine, Graduate School of Medicine, Kyoto University, Kyoto, Japan

Single nucleotide polymorphisms (SNPs) are important markers to investigate genetic heterogeneity of population and to perform linkage disequilibrium (LD) mapping. We propose a new method, Ψ, to express frequency of 2^{N_s} haplotypes for N_s di-allelic SNPs. Using the new expression of haplotype frequency, we propose a novel measure of LD, D_g, not only for SNP pairs but also for multiple markers. The values of D_g for SNP pairs were revealed to be similar to values of conventional pairwise LD indices, D' and r^2, and it was revealed that D_g quantitated components of LD that were not measured by conventional LD indices for SNP pairs. Also we propose a distinct method, D_g-based absolute estimation, to infer the absolute maximum estimates of haplotype frequency. The result of the D_g-based absolute estimation of haplotype frequency for SNP pairs were compared with the conventional expectation-maximization (EM) algorithm and reported that the new method gave better inference than the EM algorithm which converged infrequently to a local extreme. *Genet. Epidemiol.* 31:709–726, 2007. © 2007 Wiley-Liss, Inc.

*Correspondence to: Ryo Yamada, Center for Genomic Medicine, Graduate School of Medicine, Kyoto University, Kyoto, Japan.
Received 24 September 2006; Revised 27 February 2007; Accepted 29 March 2007
Published online 16 May 2007 in Wiley InterScience (www.interscience.wiley.com).
DOI: 10.1002/gepi.20235

INTRODUCTION

DNA molecules are chemical compounds that carry genetic information in living organisms. As carriers of genetic information, they have to be homogeneous enough to maintain identity of species and successful reproduction (speciation hypothesis) [Rieseberg 2001; Noor et al., 2001; Navarro and Barton, 2003; Rieseberg and Livingstone, 2003]. On the contrary, they carry heterogeneity that is believed to give benefit to species for survival in ever-changing environments (adaptation) [Hartl and Clark, 1997a]. Heterogeneity of DNA sequence in a population is balanced between pressures in the two directions, toward the homogeneity or clonality and toward the heterogeneity or randomness.

To clarify the heterogeneity of DNA sequence population, let us assume two extreme populations. In one population, all the DNA molecules are completely identical, in other words, a clonal population. In the other one, any nucleotide in the DNA molecules is randomly selected. In this random population, any site in the DNA molecules is polymorphic, and no association exists between sites or between sets of sites. We define the randomness of polymorphism of individual sites as "allele frequency-randomness" and the randomness between sites or between sets of sites as "inter-site randomness". Because only a small fraction of nucleotide sites in a species is polymorphic, the inter-site randomness is observed only among the polymorphic sites. The pressures toward the clonality of individual sites include selection by favorable phenotypes, unsuccessful reproduction through excessive discrepancy between sequences from gametes and genetic drift due to finite effective population size with unbalanced transmission. On the contrary, mutation and recombination of the genetic material to descendent increase the allele frequency randomness and the inter-site randomness [Hartl and Clark, 1997b].

Since the genome sequences from multiple organisms were determined, one of major research targets has been the investigation of intraspecies variations [Collins et al., 2003]. As reported in *Drosophila*, recombination rate seemed correlated with the presence of nucleotide polymorphisms [Aquadro et al., 1994]. Therefore the allele frequency-randomness of individual nucleotides and the inter-site randomness should be quantitated together. Unfortunately nucleotide diversity, the most popular parameter to quantify heterozygosity at the nucleotide level does not take into account the LD [Hartl and Clark, 1997c]. On the other hand, LD indices, such as D' and r^2 as well as multiallelic D' quantitate only allelic inter-site dependency [Devlin and Risch, 1995; Zapata, 2000].

Because single nucleotide polymorphisms (SNPs) are the most common variations [Kidd et al., 2004] and the LD mapping using SNPs is a very promising method to investigate genetic background of various phenotypes, [Morton, 2005], we propose a new method, Ψ, to express the allele frequency-randomness of individual sites and the intersite randomness for diallelic markers together by a uniform expression. The introduction of Ψ enables us to propose D_g as a novel measure of LD for multiple SNPs, which will be beneficial for genetic studies because only limited measures of LD for multiple loci are currently available, such as ε [Nothnagel et al., 2002], are now limited.

Also using Ψ, we propose a new method to infer the absolute maximum estimate of haplotype frequency. Although the conventional expectation-maximization (EM) algorithm is known to give a local maximum periodically [Nin, 2004], Ψ-based method enables us to overcome the shortcoming and to infer the global maximum of haplotype frequency for SNP pairs, we compared both methods and verified that the conventional EM scarcely converges to a local maximum.

INTRODUCTORY EXAMPLES

Before we give generalized expressions of Ψ and D_g, some examples are introduced.

INCOMPLETENESS OF PAIRWISE LD INDEX

Assume three SNP sites, $S = \{s_A, s_B, s_C\}$, and their eight haplotypes

$H = \{$"ABC", "ABc", "AbC", "Abc", "aBC", "aBc", "abC", "abc"$\}$.

When their haplotype frequencies are

$$F_1 = \{f_{ABC}, f_{ABc}, f_{AbC}, f_{Abc}, f_{aBC}, f_{aBc}, f_{abC}, f_{abc}\}$$
$$= \{0.125, 0.125, 0.125, 0.125, 0.125, 0.125, 0.125, 0.125\}$$

or

$$F_2 = \{0.25, 0, 0, 0.25, 0, 0.25, 0.25, 0\}$$

pairwise r^2's [Devlin and Risch, 1995] of three SNP pairs for both F_1 and F_2 are 0, because frequencies of four haplotypes for each pair are $\{0.25, 0.25, 0.25, 0.25\}$ for both cases (See Columns 1 "$F1$" and 2 "$F2$" in Table I). Although the two cases are apparently different in terms of LD, their pairwise LD index values are the same. This difference implicates that there are components of LD which three pairwise LD indices can not describe. In this article, we propose a LD measure D_g to quantitate all LD components.

CALCULATION OF Ψ AND D_g

Ψ is a novel system to express haplotype frequencies and D_g is a new measure of LD for multiple sites. From haplotype frequencies, Ψ is calculated initially, and D_g is deduced from Ψ.

Transformation of F_i to Ψ and Ψ plots. $\Psi = \{\psi_{subset}\}$ for SNP trio S has eight elements, each of which corresponds to a subset of

$$S: \{\{\phi\}(\text{empty}), \{s_A\}, \{s_B\}, \{s_C\}, \{s_A, s_B\}, \{s_A, s_C\}, \{s_B, s_C\}, \{s_A, s_B, s_C\}\}.$$

The Ψ elements for each subset are defined with frequency of their alleles (f_x: frequency of haplotype or allele "x") as below:

$$\psi_\phi = 1,$$
$$\psi_{s_A} = f_A - f_a,$$
$$\psi_{s_B} = f_B - f_b,$$
$$\psi_{s_C} = f_C - f_c,$$
$$\psi_{s_A,s_B} = f_{AB} - f_{Ab} - f_{aB} + f_{ab},$$
$$\psi_{s_A,s_C} = f_{AC} - f_{Ac} - f_{aC} + f_{ac},$$
$$\psi_{s_B,s_C} = f_{BC} - f_{Bc} - f_{bC} + f_{bc},$$
$$\psi_{s_A,s_B,s_C} = f_{ABC} - f_{ABc} - f_{AbC} + f_{Abc} - f_{aBC} + f_{aBc} + f_{abC} - f_{abc}.$$

Table I gives frequencies of three sites, three site-pairs and trio as well as the corresponding Ψs. For the case of F_1, $\Psi = \{1, 0, 0, 0, 0, 0, 0, 0\}$ and for F_2, $\Psi = \{1, 0, 0, 0, 0, 0, 0, 1\}$. The first seven elements of Ψ for both cases are the same and the last element, ψ_{s_A,s_B,s_C}, represents the difference between the two.

It is noticed that there is a rule of alternation of positive/negative signs in the expression of Ψ's with frequency of haplotypes, implicating that the expression will be generalized for more nucleotide sites as shown later in this article. Also it is noticed that the introduced variables are in the hierarchic and nested structure. In other words, the elements of Ψ for three sites are consisted of the elements of Ψ's for subsets of sites with an additional component specific to the trio. The nested structure is visualized as Ψ plots in Figure 1(a) with detailed description of its structure. The Ψ plots tell that the difference between F_1 and F_2 is located into the row on the bottom, that stands for the trio. Ψ for the trio contains Ψ for SNP pairs. The four circles in the upper left of Ψ plots, corresponding to $\psi_\phi, \psi_{s_A}, \psi_{s_B}$ and ψ_{s_A,s_B}, create a rhombus that is Ψ plot for the site-pair. Two other rhombuses for site-pairs, $\{s_A, s_C\}$ and $\{s_B, s_C\}$ exist in the Ψ plot of the trio as well. All circles except for ψ_{s_A,s_B,s_C} are a part of at least one of three rhombuses for site-pairs. Figure 1(b) shows structure of Ψ plots of one to seven sites. The Ψ plot of n sites contains Ψ plots of $n-1$ sites in its inside. All the elements in the Ψ plot of n sites except one circle at the bottom are a part of at least one of Ψ's of $n-1$ sites as shown in Figure 1(b).

Calculation of D_g from Ψ and D_g plots. D_g quantitates LD for division patterns of multiple SNPs. For example, a division, $(s_A, s_B, s_C) \rightarrow \{(s_A, s_B), (s_C)\}$ means a division of three SNPs into a SNP pair (s_A, s_B)

TABLE I. Haplotype frequencies and their ψ and D_g

	1	2	3	4	5	6	7	8	9	10	11	12	13	14
Column ID	F1	F2	Clone1	Clone2	1 SNP	2 SNPs in absolute LD	2 SNPs in LE	2 SNPs in partial LD	3 SNPs in absolute LD-1	3 SNPs in absolute LD-2	3 SNPs in LE	3 SNPs in partial LD-1	3 SNPs in partial LD-2	3 SNPs in partial LD-3
f_{ABC}	0.125	0.25	1	0	0.6	0.6	0.42	0.6	0.5	0.6	0.336	0.3	0.3	0.3
f_{ABc}	0.125	0	0	1	0	0	0	0	0	0	0.084	0	0	0
f_{AbC}	0.125	0	0	0	0	0	0.18	0.3	0	0	0.144	0	0	0
f_{Abc}	0.125	0.25	0	0	0	0	0	0	0	0	0.036	0.2	0.2	0.3
f_{aBC}	0.125	0	0	0	0.4	0	0.28	0	0	0	0.224	0.3	0.2	0.2
f_{aBc}	0.125	0.25	0	0	0	0	0	0	0	0	0.056	0	0	0
f_{abC}	0.125	0.25	0	0	0	0.4	0.12	0.1	0	0	0.096	0	0	0
f_{abc}	0.125	0	0	0	0	0	0	0	0.5	0.4	0.024	0.2	0.3	0.2
f_A	0.5	0.5	1	1	0.6	0.6	0.6	0.9	0.5	0.6	0.6	0.5	0.5	0.6
f_a	0.5	0.5	0	0	0.4	0.4	0.4	0.1	0.5	0.4	0.4	0.5	0.5	0.4
f_B	0.5	0.5	1	1	1	0.6	0.7	0.6	0.5	0.6	0.7	0.6	0.5	0.5
f_b	0.5	0.5	0	0	0	0.4	0.3	0.4	0.5	0.4	0.3	0.4	0.5	0.5
f_C	0.5	0.5	1	0	1	1	1	1	0.5	0.6	0.8	0.6	0.5	0.5
f_c	0.5	0.5	0	1	0	0	0	0	0.5	0.4	0.2	0.4	0.5	0.5
f_{AB}	0.25	0.25	1	1	0.6	0.6	0.42	0.6	0.5	0.6	0.42	0.3	0.3	0.3
f_{Ab}	0.25	0.25	0	0	0	0	0.18	0.3	0	0	0.18	0.2	0.2	0.3
f_{aB}	0.25	0.25	0	0	0.4	0	0.28	0	0	0	0.28	0.3	0.2	0.2
f_{ab}	0.25	0.25	0	0	0	0.4	0.12	0.1	0.5	0.4	0.12	0.2	0.3	0.2
f_{AC}	0.25	0.25	1	0	0.6	0.6	0.6	0.9	0.5	0.6	0.48	0.3	0.3	0.3
f_{Ac}	0.25	0.25	0	1	0	0	0	0	0	0	0.12	0.2	0.2	0.3
f_{aC}	0.25	0.25	0	0	0.4	0.4	0.4	0.1	0	0	0.32	0.3	0.2	0.2
f_{ac}	0.25	0.25	0	0	0	0	0	0	0.5	0.4	0.08	0.2	0.3	0.2
f_{BC}	0.25	0.25	1	0	1	0.6	0.7	0.6	0.5	0.6	0.56	0.6	0.5	0.5
f_{Bc}	0.25	0.25	0	1	0	0	0	0	0	0	0.14	0	0	0
f_{bC}	0.25	0.25	0	0	0	0.4	0.3	0.4	0	0	0.24	0	0	0
f_{bc}	0.25	0.25	0	0	0	0	0	0	0.5	0.4	0.06	0.4	0.5	0.5
ψ_Φ	1	1	1	1	1	1	1	1	1	1	1	1	1	1
ψ_{S_A}	0	0	1	1	0.2	0.2	0.2	0.8	0	0.2	0.2	0	0	0.2
ψ_{S_B}	0	0	1	1	1	0.2	0.4	0.2	0	0.2	0.4	0.2	0	0
ψ_{S_C}	0	0	1	−1	1	1	1	1	0	0.2	0.6	0.2	0	0
ψ_{S_A,S_B}	0	0	1	1	0.2	1	0.08	0.4	1	1	0.08	0	0.2	0
ψ_{S_A,S_C}	0	0	1	−1	0.2	0.2	0.2	0.8	1	1	0.12	0	0.2	0
ψ_{S_B,S_C}	0	0	1	−1	1	0.2	0.4	0.2	1	1	0.24	1	1	1
ψ_{S_A,S_B,S_C}	0	1	1	−1	0.2	1	0.08	0.4	0	0.2	0.048	0	0	0.2

Genet. Epidemiol. DOI 10.1002/gepi